Decentralized Demand Response for Energy Hubs in Integrated Electricity and Gas Systems Considering Linepack Flexibility

Sheng Wang, *Member, IEEE*, Hongxun Hui, *Member, IEEE*, Yi Ding, *Member, IEEE*, and Junyi Zhai, *Member, IEEE*

***Abstract*—The wide application of energy conversion facilities on the demand side, such as combined heat and power units, has accelerated the integration of multiple energy carriers in the form of energy hub (EH). EH can flexibly schedule its electricity and gas consumption patterns to provide demand response (DR) services to the electricity system. However, DR can introduce significant uncertainties in gas demands, posing challenges to the real-time balance of the integrated electricity and gas systems (IEGSs). The gas stored in the pipeline (i.e., linepack) is a promising flexible resource to accommodate the gas demand uncertainties during the DR. However, using linepack is challenging due to the complex physical characteristics of gas flow dynamics. This article proposes a coordinated optimal control framework for both EH and IEGS, focusing on leveraging the linepack flexibility to enhance DR capabilities. First, a multilevel self-scheduling framework for the EH is developed to comprehensively explore the DR potential. The gas flow dynamic constraints are then formulated to ensure that the fluctuating gas demand can be accommodated by the linepack in the IEGS. The second-order cone (SOC) relaxation is adopted to convexify the nonlinearity in the motion equation of gas flow dynamics. To tackle the overall mixed-integer SOC programming problem, an enhanced Benders decomposition strategy that incorporates the lift-and-project cutting plane method is developed, along with a novel solution procedure. The proposed method is validated using the IEEE 24-bus Reliability Test System and the Belgium natural gas transmission system to demonstrate its effectiveness.**

***Index Terms*—Demand response (DR), energy hub (EH), gas flow dynamics, integrated electricity and gas systems (IEGSs), self-schedule.**

Manuscript received 22 March 2023; revised 12 September 2023 and 30 October 2023; accepted 5 November 2023. Date of publication 8 November 2023; date of current version 26 March 2024. This work was supported in part by the Science and Technology Development Fund, Macau, SAR, under Grant SKL-IOTSC(UM)-2021-2023, Grant 0003/2020/AKP, and Grant 0117/2022/A3; and in part by the Natural Science Foundation of Jiangsu Province, China, under Grant BK20220261. *(Corresponding authors: Hongxun Hui; Junyi Zhai.)*

Sheng Wang and Hongxun Hui are with the State Key Laboratory of Internet of Things for Smart City, Department of Electrical and Computer Engineering, University of Macau, Macau, China (e-mail: shengwang@um.edu.mo; hongxunhui@um.edu.mo).

Yi Ding is with the College of Electrical Engineering, Zhejiang University, Hangzhou 310058, China (e-mail: yiding@zju.edu.cn).

Junyi Zhai is with the College of New Energy, China University of Petroleum (East China), Qingdao 266580, China (e-mail: zhaijunyi@upc.edu.cn).

Digital Object Identifier 10.1109/JIOT.2023.3331115

I. Introduction

With the increasing concern for low-carbon development, the coordinated utilization of different energies (e.g., electricity, gas, and heat) has become one of the most appealing ways to promote energy efficiency [1]. On the demand side, different energies are linked through local devices, such as combined heat and power plants (CHPs), electric heat pumps (EHPs), etc. They consume energy from both electricity and gas systems to satisfy the electricity, heating, and cooling demands of end users [2]. In response to this trend, the concept of the energy hub (EH) is developed to feature the energy conversion from multiple energy supplies to consumptions [3].

EH not only integrates multiple energies but also diversifies the path to fulfill energy demands [4]. For instance, the heating demand supplied by the EHP can be covered by increasing the heat production of the CHP, thereby reducing total electricity consumption while increasing gas consumption by the CHP. This tradeoff among different energy consumptions, known as energy substitution, can be leveraged to provide demand response (DR) service to the electricity system [5]. Some studies have explored energy substitution-based DR (the comprehensive literature review is listed in Table I). For example, it is used to flexibly supply the electrical, heating, and cooling demands for a building in [6]. Noncooperative game and Nash equilibrium are analyzed in DR considering energy substitutions of multiple EHs in [7]. The joint effect of energy substitution and load elasticity are examined in [8] considering the energy price uncertainties and incentives. A stochastic planning method is formulated as a two-stage optimization problem in [9] to optimize the EH operation and explore DR potential based on energy substitution potentials. Collaborative operations of high-renewable penetrated industrial EHs have been proposed, modeling the feasible regions of each device [10]. A block-coordinate-descent robust optimization for incentive-based DR in EH is proposed in [11] against uncertainties. Practical projects, like the test-bed plant in Spain, have further demonstrated the potential of energy substitution in EHs [12]. Compared with traditional DR in electricity systems (e.g., changing the charging/discharging patterns of electric vehicles [13], regulating the on–off statuses of air conditioners [14], etc.), energy substitution in EHs can provide a more seamless experience for end users [15], [16].

TABLE I
SUMMARY OF THE PREVIOUS STUDIES

Aspect	Model/method in previous studies	Issues remain unaddressed	References
Cooperation of multiple DR strategies in EH	Energy substitution only	Cannot fully excavate DR potential	[7-11]
	Energy substitution and load curtailment		[18, 19]
	Temporal load shifting	Cannot characterize the time-dependency in the load-shifting process	[16, 20, 21]
Coordination between EHs and IEG	Steady-state gas flow model	Cannot reflect the real-time condition of the gas system during DR	[24-28, 32, 34, 36]
	Quasi-dynamic gas flow model	Cannot reflect the gas pressure change during the utilization of linepacks	[33]
Solution of the EH-IEGS coordination problem	Nonlinear form	The computation efficiency and accuracy cannot be guaranteed	[25] [32]
	Linearization around the average gas flow point	The accuracy cannot be guaranteed considering the gas demand spikes during the DR	[33]
	Piecewise linearization	The computation efficiency and accuracy cannot be well balanced	[27, 28, 34]
	Second-order cone relaxation	The previous studies have not applied the second-order cone relaxation to the dynamic gas flow model yet	[35, 36]
	Other decentralization-based methods	Models do not consider time interdependency, so their methods are difficult to be applied directly in this paper	[37]

However, there are three main challenges regarding the provision of DR in EHs.

A. Multistrategy Cooperation

Energy substitution is one of several flexible DR strategies available in EHs. Strategies, such as temporal load shifting and initiative load curtailment, have proven effective in reducing peak loads and flattening load curves in traditional electricity systems [17]. Previous studies have attempted to incorporate these strategies into DR in EHs but often with simplified models. For example, some studies divide energy loads into fixed, interrupted, and adjusted loads, where the adjusted load is regulated by changing the setting temperature of thermal-controlled loads [18]. The cooperation strategy between CHP and curtailable air condition loads has been investigated [19]. Flexible energy loads are classified as primary and deferrable loads, but the latter does not need to be recovered mandatorily [20]. The load shifting process in [21] only forces the balance of shift-out and shift-in loads within a long period, while the real-time balance and time interdependency in the load shifting are not considered.

In summary, Existing temporal load-shifting models cannot capture the time interdependency of load-shifting processes accurately. Furthermore, the full potential of DR using cooperative multistrategy approaches remains untapped. However, incorporating time-dependent temporal load shifting increases the computational complexity of the EH scheduling problem, necessitating efficient modeling, and solution methodologies.

B. Multisystem Coordination

Generally, multiple EHs can exist at different locations on the demand side, consuming electricity, and gas from integrated electricity and gas systems (IEGSs) to meet their energy demands. During DR, energy substitution in EHs may lead to a spike in gas demand, which could impact the normal operation of the gas system [22]. Linepack, the gas stored in pipelines, represents a flexible resource that can accommodate gas demand spikes during DR due to its accessibility and quick response [23]. Previous studies have addressed the coordination of EHs and IEGS using steady-state gas flow models. For example, the probabilistic energy flow of IEGS with renewable-based EH is investigated in [24]. An optimal operation of electricity, natural gas, and heat systems considering integrated DR and diversified storage devices is developed in [25]. The uncertainties of renewable energies and electricity/gas demand are incorporated in [26] in a stochastic day-ahead scheduling framework. The day-ahead market framework is further considered in [27] and modeled as a mixed-integer nonlinear programming problem. A distributed planning model of IEGS and EHs is proposed in [28] in the long term.

However, existing steady-state gas flow-based frameworks fail to fully utilize the flexibilities offered by linepack during DR. Some studies have investigated the linepack utilization for optimal dispatch [29], resilience management [30], etc., but its application in DR and the coordination with EHs remains unexplored. Modeling linepack usage requires adherence to the physical laws of gas flow dynamics, which are highly time-dependent [31]. Thus, coordinating linepack and EH scheduling during real-time DR poses significant challenges, necessitating a new framework for enhanced coordination.

C. Problem Tractability

As aforementioned, Incorporating various DR strategies and gas flow dynamics into the optimization of IEGS and EHs creates a large-scale, time-dependent, and nonlinear optimal control problem. These characteristics make traditional centralized solution methods less efficient or robust. In previous research, where coordination problems were typically time-independent and of smaller scale, centralized solution methods sufficed. For example, some studies retained the nonlinear form of the optimization problem and solved it using solvers like IPOPT [25] or heuristic algorithms [32]. Others convexified the problem by linearizing the quadric term of gas flow equations around the normal operating point [33]. Piecewise linearization and second-order cone (SOC) relaxation techniques were also employed [34], [35]. While a few studies adopted decentralized solution methods for the joint dispatch of IEGS and EHs, they were found to be less efficient than traditional centralized methods [36].

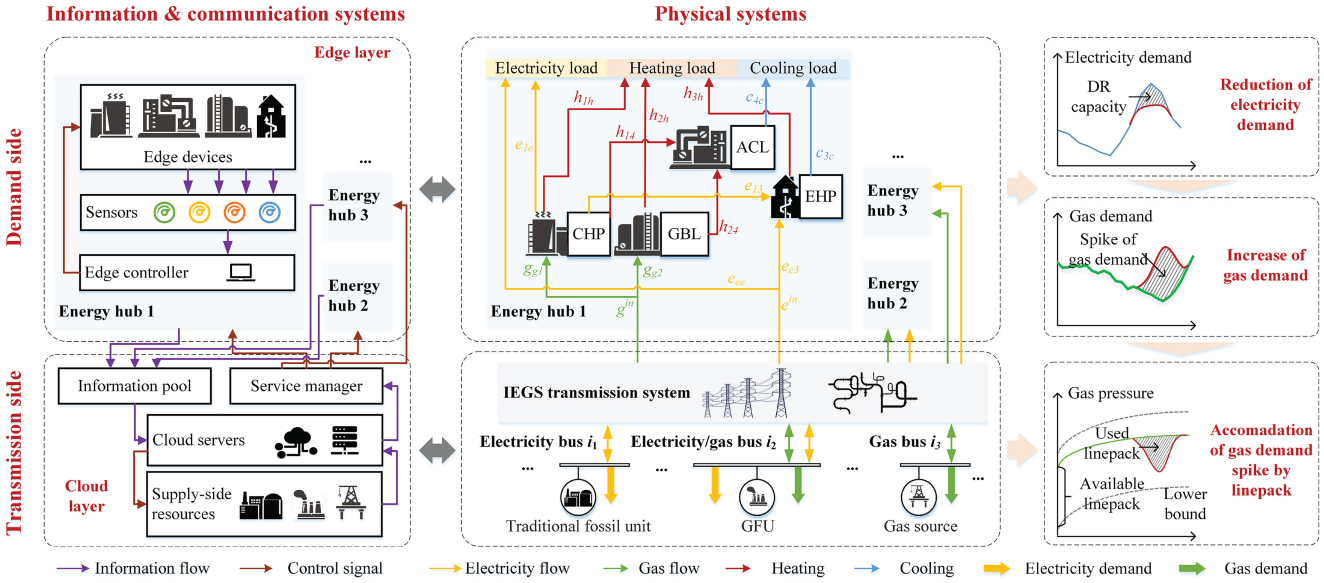

Fig. 1. Coordination framework of the IEGS and EHs for providing DR by using linepack.

In summary, previous studies primarily focused on energy substitution strategies and steady-state gas flow models in EHs and IEGS, respectively, which did not fully address the scale and time interdependency challenges encountered in DR optimization models. Consequently, existing solution methods cannot be directly applied to the proposed DR problem, necessitating a new solution strategy.

To address the above research gaps, this article proposes a decentralized DR framework for IEGS and EHs. The contributions are summarized as follows.

1) A multilevel self-scheduling model for the EH is proposed to exploit DR potential. Compared with previous studies, the proposed model can cooperate the energy substitution, load shifting, and initiative load curtailment strategies. By employing the McCormick envelope, the time interdependency in load shifting is characterized more accurately and tractably.
2) A coordinated optimal control framework of the IEGS and EHs is proposed for providing DR service. Compared with the traditional steady-state-based framework, this approach leverages linepack flexibilities to accommodate gas demand spikes during DR. The SOC relaxation is tailored to convexity the gas flow dynamic equations, so that it can be addressed by off-the-shelf solvers.
3) An enhanced Benders decomposition is developed to solve the coordinated optimal control problem in a decentralized manner to protect privacy. The Lift-and-project (L&P) cutting plane method is embedded to handle integer variables in subproblems. Additionally, a novel solution procedure is designed, leveraging the multilevel structure of the EH self-scheduling problem to enhance computational efficiency.

II. Structure of the IEGS and EHs

The structure of the IEGS and EHs is presented in Fig. 1. It contains two systems, i.e., the physical system and the information and communication system (ICT). The physical system is further divided into the transmission side and the demand side. On the transmission side, the IEGS transports the electricity and gas from generating units (such as gas-fired generating units (GFUs) and traditional fossil units) and gas sources (such as gas wells and storages) to the demand side, respectively. The GFU consumes gas to generate electricity, acting as a crucial link between the gas and electricity systems [38]. On the demand side, districts, such as the campus, industrial park, and buildings, can be modeled as EHs [39]. In this article, a typical configuration of the EH is considered, including the CHP, gas boiler (GBL), EHP, and absorption chiller (ACL).

In addition to the physical system, an ICT-based cloud–edge computing framework is devised to implement the proposed decentralized control framework [40]. The demand side corresponds to the edge layer, where EH devices like CHP, GBL, etc., act as edge devices. These devices, along with end users, are equipped with various sensors to measure output and environmental states, such as temperature [41], [42]. The collected data are transmitted to the edge controller to implement a self-scheduling strategy. Furthermore, essential EH information is shared with the cloud layer to make centralized and globally optimal decisions. The cloud servers gather information and dispatch EHs as well as supply side resources such as generators. It is important to note that due to the decentralized control framework, only minimal information is exchanged to preserve privacy.

Figs. 1 and 2 jointly depict the implementation process of DR. During operation, DR instructions, including the electricity reduction period and capacity, are broadcast to each EH. Based on these instructions, EHs implement multilevel self-scheduling to provide the required DR service for the specified period. Self-scheduling strategies, such as energy substitution, load shifting, and load curtailment, are implemented at different time intervals, as shown in Fig. 2. The self-scheduling of EHs effectively reduces electricity demand, although it may

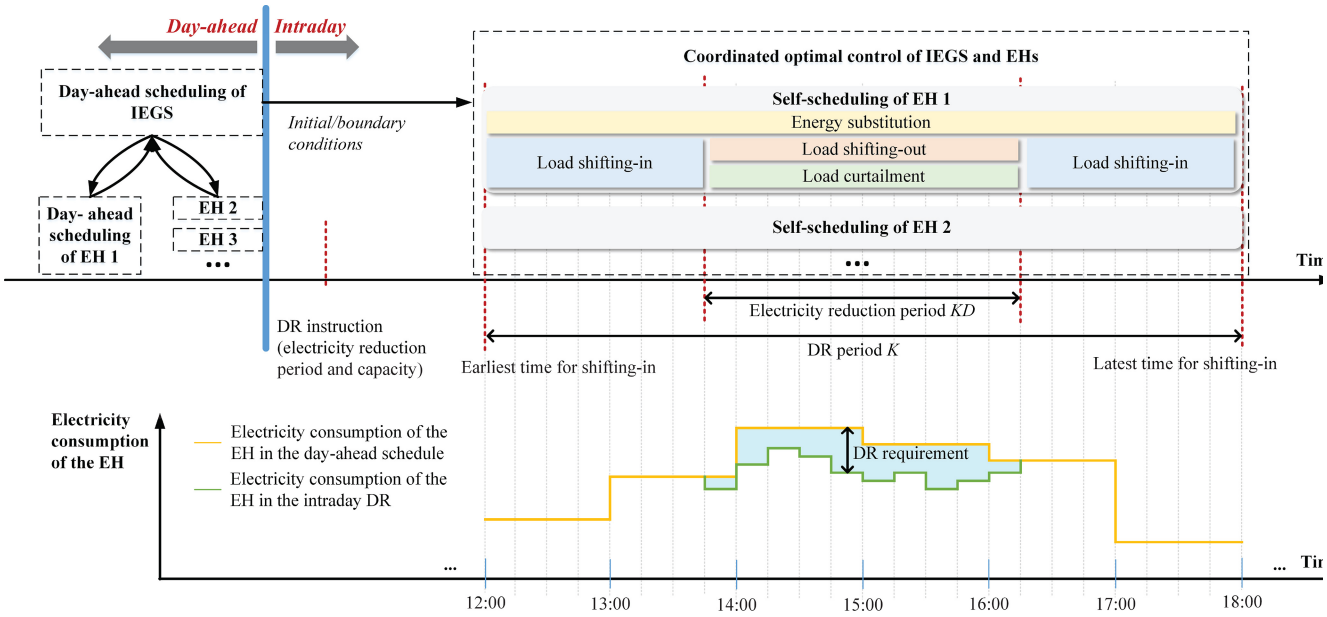

Fig. 2. Implementation timeline of DR in the IEGS and EHs.

lead to a significant increase in gas demand. To address this, the linepack in the gas pipeline can temporarily accommodate the gas demand spike by lowering the gas pressure within the secure range. Therefore, considering the physical interaction between IEGS and EHs, a coordination framework is essential to provide DR service in a globally optimal manner.

III. Multilevel Self-Scheduling Model of the EH

The operating schedule of the EH is typically determined in the day-ahead to satisfy the forecasted electricity, heating, and cooling loads. The DR instruction can be broadcast to the EH either in the day-ahead or during intraday operation. Upon receiving the instruction, the EH implements a self-scheduling strategy to adjust its operating conditions and fulfill the DR requirements [43]. Therefore, both day-ahead scheduling and intraday self-scheduling are studied in this section.

A. Optimal Scheduling of the EH in the Day-Ahead

The objective of the optimal scheduling in the day-ahead is to minimize the energy purchasing cost C_{EH} on an hourly basis

$$\min_{e^{in},g^{in},\mathbf{x}^{st}} C_{\mathrm{EH}} = \rho^{e} \times e^{in} + \rho^{g} \times g^{in} \tag{1}$$

where e^{in} and g^{in} are the electricity and gas consumptions of the EH, respectively; ρ^{e} and ρ^{g} are the nodal electricity and gas prices, respectively, which can be obtained as constants by solving the optimal economic dispatch problem of IEGS in the day-ahead with forecast electricity and gas loads [44].

The objective function is subject to the following.

1) Energy Conversion Equations: The following equations characterize the energy conversion relations between the state variables (including electricity and gas consumption and energy output of devices $\mathbf{x}^{st}$=[g_{g1}, g_{g2}, e_{ee}, e_{e3}, e_{1e}, e_{13}, h_{1h}, h_{14}, h_{2h}, h_{24}, c_{3c}, h_{3h}, c_{4c}], as marked in Fig. 1) and energy loads in the EH

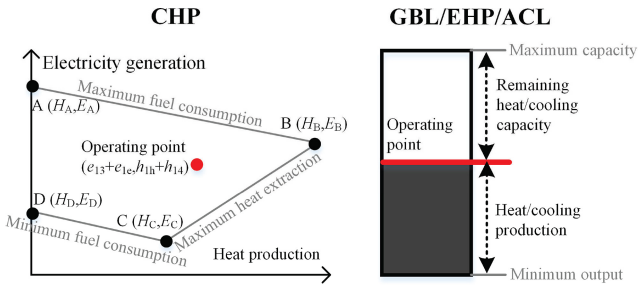

Fig. 3. Feasible regions of EH devices.

$$\mathbf{H}_{11\times 15}\left[e^{in}\ g^{in}\ \mathbf{x}^{st}\right]^{T} = \left[d^{el}\ d^{ht}\ d^{cl}\ \mathbf{0}_{1\times 8}\right]^{T} \tag{2}$$

$$\mathbf{x}^{st} \geq 0 \tag{3}$$

where $\mathbf{H}$ is the sparse energy conversion matrix, whose specific form can be found in the Appendix; el, *ht*, and cl represent the energy types of electricity, heat, and cooling, respectively; and d^{el}, d^{ht}, and d^{cl} are the electricity, heat, and cooling loads of the EH, respectively. For example, the ACL constraint in (2) can be written as

$$\left(h_{1,4} + h_{2,4}\right)\mathrm{COP}_4 - c_{4,c} = 0. \tag{4}$$

It means that by consuming the heat energies from CHP $h_{1,4}$ and GBL $h_{2,4}$, the ACL can provide $c_{4,c}$ cooling energy to the cooling load at the efficiency of COP_4.

2) CHP Constraints: The electricity generation and heat production of the CHP have interdependencies. The feasible region of the CHP can be represented by a convex quadrangle area, as shown in the left half of Fig. 3 [10]. A, B, C, and D are the four extreme points that define the quadrangle. Their coordinates of heat production and electricity generation are (H_A,E_A), (H_B,E_B), (H_C,E_C), and (H_D,E_D). Therefore, the

feasible region of the CHP can be expressed by four linear constraints

$$h_{1h} + h_{14} \geq 0 \quad (5)$$

$$e_{13} + e_{1e} - E_A - \frac{E_A - E_B}{(H_A - H_B)(h_{1h} + h_{14})} \leq 0 \quad (6)$$

$$e_{13} + e_{1e} - E_B - \frac{E_B - E_C}{(H_B - H_C)(h_{1h} + h_{14} - H_B)} \geq 0 \quad (7)$$

$$e_{13} + e_{1e} - E_D - \frac{E_C - E_D}{(H_C - H_D)(h_{1h} + h_{14})} \geq 0. \quad (8)$$

3) GBL, EHP, and ACL Constraints: The heat/cooling outputs of GBL, EHP, and ACL are subject to the minimum outputs and maximum capacities of these devices, as shown in the right half of Fig. 3

$$ho_2^- \leq h_{24} + h_{2h} \leq ho_2^+ \quad (9)$$

$$co_4^- \leq c_{4c} \leq co_4^+ \quad (10)$$

$$\gamma ho_3^- \leq h_{3h} \leq \gamma ho_3^+ \quad (11)$$

$$(1-\gamma) co_3^- \leq c_{3c} \leq (1-\gamma) co_3^+ \quad (12)$$

where ho_2^+, ho_3^+, co_3^+, and co_4^+ are the heating/cooling capacities of GBL, EHP, and ACL, respectively; ho_2^-, ho_3^-, co_3^-, and co_4^- are the minimum heating/cooling outputs of these devices, respectively; and γ is the indicator for EHP operating mode, where $\gamma = 1$ represents heating mode, and $\gamma = 0$ represents cooling mode.

The optimal schedule in the day-ahead should be formulated for each EH in each hour. Denote the solutions for the nth EH in the hth hour as $e_{n,h}^{in*}$, $g_{n,h}^{in*}$, $\mathbf{x}_{n,h}^{st*}$.

B. Multilevel Self-Scheduling of the EH in the Intraday

During the intraday operation, the EH can implement the multilevel self-scheduling strategy to provide DR capacity, namely, energy substitution, temporal load shifting, and load curtailment, as illustrated in Fig. 4. From the first to the third level strategy, the EH can provide more DR capacity, but the cost will be higher. The three strategies are elaborated as follows.

1) First-Level Strategy (Energy Substitution): Energy substitution is to provide DR capacity by changing the operating point of the devices in the EH, as shown in the first figure in Fig. 4. In this strategy, the interruption to the energy loads can be minimized. The specific strategy can take different forms. For example, 1) increase the electricity generation of CHP by consuming more gas or by reducing its heat production and 2) decrease the heat production of EHP, and increase the heat production of GBL if it is winter. By implementing these strategies, the electricity consumption of EH can be reduced, and the DR capacity can be provided.

The control variables of the energy substitution include the electricity consumption e^{in}, the gas consumption g^{in}, and the state variables $\mathbf{x}^{st}$ of the EH. Apart from the same constraints (2)–(12) in the day-ahead scheduling, energy substitution should consider the DR capacity requirement. As shown in the bottom half of Fig. 2, the yellow line represents the electricity consumption of the EH in the day-ahead schedule $e_{n,h}^{in*}$. During the DR period K, the requirement of

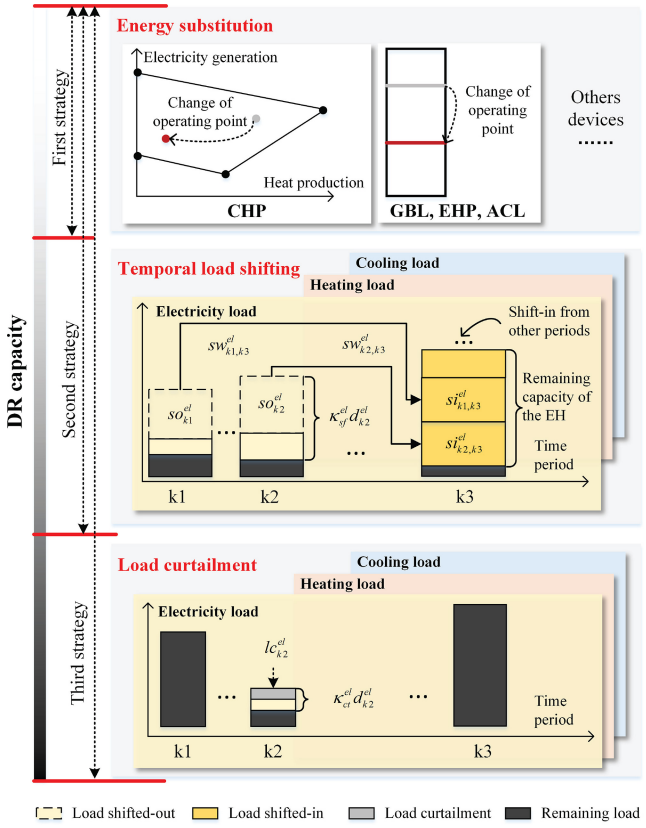

Fig. 4. Multilevel self-scheduling strategy of the EH.

DR capacity for each EH n in each time period k (i.e., $ER_{n,k}$) is instructed by the system operator. Then, the electricity consumption of the EH after the DR in the intraday (i.e., $e_{n,k}^{in}$) should be lower than the green line

$$e_{n,k}^{in} \leq e_{n,h}^{in*} - ER_{n,k}, k \in K. \quad (13)$$

2) Second-Level Strategy (Temporal Load Shifting): Temporal load shifting is to shift the energy loads among time periods to adjust the load curves, and thus reduce the electricity consumption at a given time period to provide DR capacity. For example, as presented in the second figure in Fig. 4, the electricity load so_{k1}^{el} at time period $k1$ and the electricity load so_{k2}^{el} at time period $k2$ are shifted to time period $k3$. By this means, the DR capacity can be provided at time periods $k1$ and $k2$, while causing certain delays to the energy loads. This temporal load shifting can also take various forms in practice. For example, industrial users can rearrange their production plan, or residential users can reschedule their household appliances.

The temporal load shifting can be divided into two subprocesses: 1) shift-out and 2) shift-in. The shift-out process is implemented in the electricity reduction period KD, as marked in Fig. 2. The available period for shifting-in KN (KN = K − KD) should coincide with the users' preferences. For example, the shifted-out tasks (e.g., production plan) must be completed before the off-work time (e.g., 17:00). Then, the latest time for shifting-in will be 17:00. Moreover, the duration for completing the tasks should be limited within SW_k^l. Thus,

the whole temporal load-shifting process can be described as

$$\sum_{k' \in \mathrm{KN}} sw^{l}_{k,k'} = SW^{l}_{k}, \forall k \in \mathrm{KD}, sw^{l}_{k,k'} \in \{0,1\} \quad (14)$$

$$so^{l}_{k} = \sum_{k' \in \mathrm{KN}} sw^{l}_{k,k'} si^{l}_{k,k'}, k \in \mathrm{KD} \quad (15)$$

$$0 \le si^{l}_{k,k'} \le so^{l}_{k} \quad (16)$$

$$0 \le so^{l}_{k} \le \kappa^{l}_{\mathrm{sf}} d^{l}_{k} \quad (17)$$

where $sw^{l}_{k,k'}$ is a binary variable denoting whether the load of energy type l in period k is deployed tok'; so^{l}_{k} is the quantity of the shifted-out load of energy type l in period k; $si^{l}_{k,k'}$ is the quantity of the energy load l shifted from period $k$to k'; and κ^{l}_{sf} is the maximum proportion of the shiftable load for energy type l.

Compared with the first-level strategy, temporal load shifting can lead to external economic losses, for it causes temporary interruption to energy loads. The economic loss of the whole temporal load shifting depends on three factors: 1) the quantity of shifted load; 2) the time interval between the shift-out and shift-in subprocesses; and 3) the unit cost for load interruption. The relation between the last two factors can be quantified using customer damage functions [45]. The customer damage function is widely used and validated to be effective in electricity system planning, operation, etc. Based on the customer damage function of the electricity load, the customer damage functions of other types of energy loads can also be derived [46]. Therefore, the cost of the temporal load shifting can be calculated as

$$C^{nd} = \sum_{k \in \mathrm{KD}} \sum_{k' \in \mathrm{KN}} \sum_{l \in \{\mathrm{el}, ht, \mathrm{cl}\}} sw^{l}_{k,k'} si^{l}_{k,k'} \mathrm{CDF}^{l}\left(\left|k' - k\right|\right) \quad (18)$$

where CDF^{l} is the customer damage function for energy type l.

3) Third-Level Strategy (Load Curtailment): If the shifted-out load in the second-level strategy cannot be redeployed within the same day or has never been redeployed, then it can be regarded as a load curtailment. As shown in the third figure in Fig. 4, the electricity load lc^{el}_{k2} is curtailed at time period $k2$. Then, the DR capacity can be provided at time period $k2$.

During the load curtailment, the curtailed load of energy type l in period k is denoted as lc^{l}_{k}. Then, it should be limited within the given boundaries

$$0 \le lc^{l}_{k} \le \kappa^{l}_{\mathrm{ct}} d^{l}_{k} \quad (19)$$

where κ^{l}_{ct} is the maximum proportion of the curtailable load of energy type l. Moreover, the customer damage function is also used to calculate the cost

$$C^{rd} = \sum_{k \in \mathrm{KD}} \sum_{l \in \{\mathrm{el}, ht, \mathrm{cl}\}} lc^{l}_{k} \mathrm{CDF}^{l}. \quad (20)$$

Summarizing all three strategies, we find that only the second strategy (i.e., temporal load shifting) is time-dependent. For example, if the load at the current time period k' is shifted into another period k, the load at the period k will be increased. Then, the original load d^{l}_{k} should be updated to load $\widetilde{d}^{l}_{k}$

$$\widetilde{d}^{l}_{k} = \begin{cases} d^{l}_{k} - so^{l}_{k} - cl^{l}_{k}, k \in \mathrm{KD} \\ d^{l}_{k} + \sum_{k' \in \mathrm{KD}} sw^{l}_{k,k'} si^{l}_{k',k}, k \in \mathrm{KN} \end{cases} \quad (21)$$

which should also meet (2)–(12).

The formulation of the above self-scheduling strategy will be integrated into the optimization model in Section V. However, the bilinear terms in (15) will lead to a mixed-integer nonlinear programming problem. Solving mixed-integer nonlinear programming problems is extremely time consuming and has no off-the-shelf reliable solvers. By using the McCormick envelope, we introduce an auxiliary variable $\chi^{l}_{k,k'} = sw^{l}_{k,k'} si^{l}_{k',k}$ to eliminate the bilinear terms [47]

$$0 \le \chi^{l}_{k,k'} \le sw^{l}_{k,k'} \kappa^{l}_{\mathrm{sf}} d^{l}_{k} \quad (22)$$

$$\chi^{l}_{k,k'} \le si^{l}_{k',k} \quad (23)$$

$$si^{l}_{k,k'} - \kappa^{l}_{\mathrm{sf}} d^{l}_{k}\left(1 - sw^{l}_{k,k'}\right) \le \chi^{l}_{k,k'} \le \kappa^{l}_{\mathrm{sf}} d^{l}_{k}. \quad (24)$$

IV. IEGS Model Considering Linepack Flexibilities

The self-scheduling strategy for EHs may lead to temporary spikes in the gas demands of IEGS. Unlike the electricity system that needs real-time balance, the spikes in gas demands can be covered by the gas stored in the transmission pipeline, which is also known as the linepack [22]. However, excessive abuse of linepacks could lower the pressure on adjacent gas buses and threaten the normal operation of the IEGS. To address this issue, this section first introduces the optimal day-ahead scheduling of IEGS to calculate the IEGS status, which can be further used to evaluate the available linepack. Then, the gas flow dynamics are modeled to ensure the security of IEGS after utilizing the linepack during the intraday DR.

A. Optimal Scheduling of IEGS in the Day-Ahead

The optimal scheduling of the IEGS is implemented on an hourly basis. The objective is to minimize the operating costs

$$\min_{w_i, g_{i,j}, g^{gfu}_{i,j}} C^{\mathrm{IEGS}} = \sum_{i \in \mathrm{GB}} \rho^{gs}_{i} w_i + \sum_{i \in \mathrm{EB}} \sum_{j \in NG_i} f^{cst}_{i,j}\left(g_{i,j}\right) \quad (25)$$

s.t.

$$w^{-}_{i} \le w_i \le w^{+}_{i} \quad (26)$$

$$g^{-}_{i,j} \le g_{i,j} \le g^{+}_{i,j} \quad (27)$$

$$g^{gfu,-}_{i,j} \le g^{gfu}_{i,j} \le g^{gfu,+}_{i,j} \quad (28)$$

$$w_i - q^{d}_{i} - \sum_{n \in EH_i} g^{in*}_{n} - \sum_{j \in NG^{gfu}_{i}} g^{gfu}_{i,j}/\xi_{i,j} - \sum_{j \in \Omega^{g}_{i}} q_{ij} = 0 \quad (29)$$

$$\sum_{j \in NG^{gfu}_{i}} g^{gfu}_{i,j} + \sum_{j \in NG_i} g_{i,j} - e^{d}_{i} - \sum_{n \in EH_i} e^{in*}_{n} - \sum_{j \in \Omega^{e}_{i}} f_{ij} = 0 \quad (30)$$

$$q_{ij} = C_{ij}\ \mathrm{sgn}\left(p_i - p_j\right)\sqrt{\left|p_i{}^2 - p_j{}^2\right|} \quad (31)$$

$$f_{ij} = (\theta_i - \theta_i)/X_{ij} \quad (32)$$

$$\left|f_{ij}\right| \le f^{+}_{ij} \quad (33)$$

$$\left|q_{ij}\right| \le q^{+}_{ij} \quad (34)$$

where C^{IEGS} is the operating cost of IEGS; ρ^{gs}_{i} is the gas purchasing price; w_i is the gas production at bus i; $g_{i,j}$ is the electricity generation of traditional fossil generating units (not gas-fueled) j at bus i; $f^{cst}_{i,j}$ is the generation cost function for traditional fossil generating units; EB and GB are the sets of electricity and gas buses, respectively; NG_i and NG^{gfu}_{i}

are the sets of traditional fossil generating units and GFU at bus$i$, respectively; q_i^d and e_i^d are the gas and electricity demands excluding EHs, respectively; $\zeta_{i,j}$ is the efficiency of the GFU; EH_i is the set of EHs at bus$i$; Ω_i^e and Ω_i^g are the sets of electricity branches and gas pipelines connected to bus i, respectively; f_{ij} and q_{ij} are the electricity and gas flows from bus i to j, respectively; θ_i is the phase angle; X_{ij} is the reactance of the branch; C_{ij} is a characteristic parameter of the pipeline, which depends on the length, absolute rugosity, and some other properties [48]; and $\mathrm{sgn}(x)$ is the signum function, where $\mathrm{sgn}(x) = 1$ if $x \geq 0$, and $\mathrm{sgn}(x) = -1$ if $x < 0$.

Denote the solution of this problem at the hth hour as $\mathbf{y}_h^{st*} = [w_{i,h}^*, g_{i,j,h}^*, g_{i,j,h}^{gfu*}]$. Denote the solution of nodal gas pressure at bus i as p_i^*. Denote the nodal electricity and gas prices as ρ_i^{e*} and ρ_i^{g*} at bus i, respectively.

B. Modeling of Gas Flow Dynamics for the Linepack Utilization in the Intraday

To ensure the security of linepack utilization during the DR, the gas flow dynamics are modeled. The gas flow dynamics in a pipeline are governed by two partial derivative equations (PDEs), namely, continuity and motion equations [49]

$$\rho_0 B^2 \partial_x q + A \partial_t p = 0 \tag{35}$$

$$\partial_x p + \rho_0 \partial_t q + \frac{2\rho_0^2 B^2 A}{F^2 D A^2 p} q|q| = 0 \tag{36}$$

where B is the isothermal wave speed of gas; ρ_0 is the gas density at the standard temperature and pressure; A is the cross-sectional area of the pipeline; D is the diameter of the pipeline; and F is the *Fanning* transmission factor.

The derivative regarding the time domain has little influence on the accuracy of (36), especially in the transmission pipelines with relatively steady flow rates and large capacities [50]. The above PDEs for the pipeline from bus i to j (the notation ij is omitted) can be discretized using the Wendroff formula [49]

$$\begin{aligned}&\Delta x A\left(p_{m+1,k+1} + p_{m,k+1} - p_{m+1,k} - p_{m,k}\right) \\ &\quad + \Delta t \rho_0 B^2 \left(q_{m+1,k+1} - q_{m,k+1} + q_{m+1,k} - q_{m,k}\right) = 0 \end{aligned} \tag{37}$$

$$\begin{aligned}&\left(p_{m+1,k+1} + p_{m+1,k}\right)^2 - \left(p_{m,k+1} + p_{m,k}\right)^2 \\ &\quad + \frac{\Delta x \Gamma \rho_0 B^2}{F^2 D A^2} \left(q_{m+1,k+1} + q_{m+1,k} + q_{m,k+1} + q_{m,k}\right)^2 = 0 \end{aligned} \tag{38}$$

where Δx and Δt are the step sizes in length and time domains, respectively; m is the index of pipeline segments; and $\Gamma = \mathrm{sgn}(q_{ij}^*)$ represents the direction of the gas flow in the day-ahead.

Assume the gas flow does not change direction during the DR period [51]. Then, (38) can be further relaxed into SOC constraints

$$\begin{cases} \left\| \begin{array}{l} p_{m,k+1} + p_{m,k},\ \frac{\rho_0 B}{\mathrm{FA}} \sqrt{\frac{\Delta x}{D}} \left(q_{m+1,k+1}\right. \\ \left. + q_{m+1,k} + q_{m,k+1} + q_{m,k}\right) \end{array} \right\| \\ \quad \leq p_{m+1,k+1} + p_{m+1,k},\ \Gamma = 1 \\ \left\| \begin{array}{l} p_{m+1,k+1} + p_{m+1,k},\ \frac{\rho_0 B}{\mathrm{FA}} \sqrt{\frac{\Delta x}{D}} \left(q_{m+1,k+1}\right. \\ \left. + q_{m+1,k} + q_{m,k+1} + q_{m,k}\right) \end{array} \right\| \\ \quad \leq p_{m,k+1} + p_{m,k},\ \Gamma = -1 \end{cases} \tag{39}$$

where penalty factor methods and sequential programming techniques can be used to drive the above relaxation tight [36].

Nodal gas pressure is the main factor that limits the utilization of linepack, which should be controlled within the secure limits during the DR period as (40). After formulating dynamic equations for all the pipelines, the initial conditions for those PDEs are specified as (41) and (42). For a set of connected pipelines, the boundary conditions are specified as (43) and (44)

$$p_i^- \leq p_i(x,t) \leq p_i^+ \tag{40}$$

$$p_{ij}|\_t = 0 = \frac{1}{C_{ij}} \sqrt{\frac{p_i^{*2} - sgn\left(p_i^* - p_j^*\right) q_{ij}^{*2} x}{L_{ij}}} \tag{41}$$

$$q_{ij}|\_t = 0 = q_{ij}^* \tag{42}$$

$$\begin{cases} p_{ij}|\_x = 0 = p_{ij_1}|\_x = 0 \left(\forall j_1 \in \Omega_i^g\right) \\ p_{ij}|\_x = 0 = p_{j_2 i}|\_x = L_{ij} \left(\forall j_2 \in \Omega_i^g\right) \end{cases} \tag{43}$$

$$\begin{aligned} &w_{i,h}^* - q_i^d - \sum_{j \in NG_i^{gfu}} \frac{g_{i,j}^{gfu}}{\xi_{i,j}} - \sum_{n \in EH_i} g_n^{in} \\ &\quad + \sum_{j \in \Omega_i^g} q_{\mathrm{ji}}|\_x = L_{\mathrm{ji}} - \sum_{j \in \Omega_i^g} q_{ij}|\_x = 0 = 0 \end{aligned} \tag{44}$$

where L_{ij} is the length of the pipeline from bus i to bus j.

V. Coordinated Optimal Control of IEGS and EHs

A. Formulation of the Coordinated Optimal Control Problem

As shown in Sections III and IV, the operating conditions of EHs are tightly coupled with IEGS. Hence, a coordinated optimal control of IEGS and EHs is required. The objective is to minimize the total cost C^T

$$\min_{\substack{p_{i,j,m,k}, q_{i,j,m,k}, g_{i,j,k}, \\ g_{i,j,k}^{gfu}, e_{n,k}^{in}, g_{n,k}^{in}, \mathbf{x}_{n,k}}} C^T = C^E + \sum_{i \in \mathrm{EB}} \sum_{n \in EH_i} \left(C_n^{nd} + C_n^{rd}\right) \tag{45}$$

$$\begin{aligned} C^E = &\sum_{k \in K} \left(\sum_{i \in \mathrm{EB}} \left(\sum_{j \in NG_i} f_{i,j}^{cst}\left(g_{i,j,k}\right) \right) \right) \\ &+ \sum_{k \in K} \left(\sum_{i \in \mathrm{EB}} \left(\rho_{i,k}^{g*} \left(\sum_{n \in EH_i} g_{n,k}^{in} + \sum_{j \in NG_i^{gfu}} g_{i,j,k}^{gfu} / \xi_{i,j} \right) \right) \right) \end{aligned} \tag{46}$$

where C^E is the energy cost; C_n^{nd} and C_n^{rd} are the costs of the temporal load shifting and load curtailment of the nth EH, respectively; $\mathbf{x}_{n,k} = [\mathbf{x}_{n,k}^{st}, \mathbf{x}_{n,k}^{nd}, \mathbf{x}_{n,k}^{rd}]$ is the set of control variables of the nth EH in period k; and $\mathbf{x}_{n,k}^{nd} = [so_{n,k}^l, si_{n,k,k'}^l,$

$sw^{l}_{n,k,k'}$, $\chi^{l}_{n,k,k'}$], $\forall k' \in \mathrm{KN}; \mathbf{x}^{rd}_{n,k} = lc^{l}_{k}$. The optimization model is subject to the following.

1) EH Operating Constraints (2)–(13): The load on the right-hand side of (2) should be replaced by the updated load $\tilde{d}^{l}_{k}$, as calculated in (21).

2) EH Self-Scheduling Constraints (14)–(24): Both EH operating and self-scheduling constraints should be formulated for all the EHs and all the time periods.

3) IEGS Operating Constraints: 1) Constraints for the gas system (37), (39)–(44), which should be formulated for all the pipelines at all the time periods; b) constraints for the electricity system (30), (32), and (33), which should also be formulated for all the periods; and c) other trivial constraints (26), (27), and (34).

B. Decentralized Solution Methodology

The IEGS and each EH generally belong to different entities and have their own regulations. To preserve their data privacies, these entities do not intend to share their system parameters [52]. Therefore, a decentralized solution strategy based on Benders decomposition is proposed.

First, through reformulating the nonlinear constraints in the optimization models in (22)–(24) and (39), the original complex problem has been preliminarily simplified into a mixed-integer SOC programming problem. Then, considering the mathematical models of the IEGS and EHs are only linked via the electricity and gas consumptions, the decomposed structure is developed. The original optimization problem is decomposed into an IEGS optimal control problem [i.e., the master problem (MP)] and several EH self-scheduling subproblems (SP). They are handled by edge and cloud computation resources, respectively. Each EH solves the subproblem individually. For privacy preservation, only the total electricity and gas consumptions and dual variables, are required to be sent to the cloud server. Thus, the detailed physical parameters of EH devices, such as the capacity of the CHP, do not have to be revealed. After the cloud server solves the MP, it will pass additional constraints to the EHs. EH will repeat the solution process of subproblems again before it converges, and thus completes our proposed decentralized Benders decomposition algorithm.

Due to the integer variables in the SPs, the Benders decomposition cannot be adopted straightforwardly. Therefore, it is enhanced by embedding the lift-and-project (L&P) cutting plane method into the SPs, so that they can be convexified. However, introducing the L&P cuts will increase the computation burden on solving the SPs. To address this issue, the enhanced Benders decomposition procedure is improved by further splitting the EH self-scheduling SP into two SPs: 1) energy substitution SP and 2) load shifting-curtailing SP. The detailed solution procedure is presented in Fig. 5, which is also elaborated as follows.

1) Initialization: Set the upper bound $\mathrm{UB}^{(0)}$, lower bound $\mathrm{LB}^{(0)}$, and tolerance δ for the enhanced Benders decomposition.

2) Solve the MP: Solve the following optimization problem to get a tentative solution for IEGS in this iteration

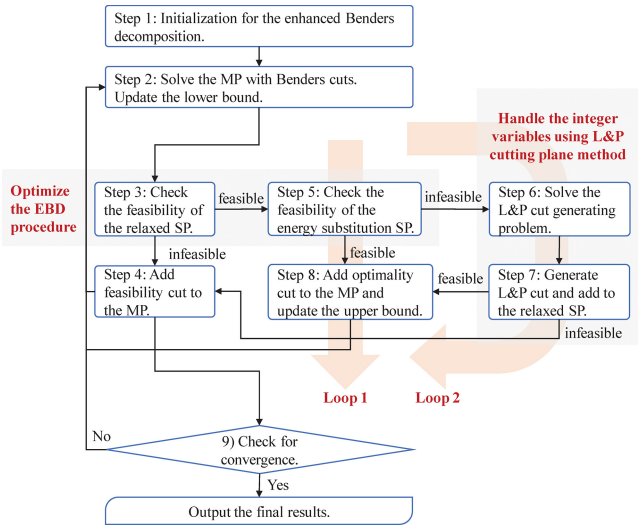

Fig. 5. Solution procedure of the enhanced Benders decomposition.

$$\underset{\mathbf{y}}{\mathrm{Min}} \quad \psi = C^{E} + \sum_{n \in \mathrm{EH}} \psi_n \tag{47}$$

where $\mathbf{y}=[p_{i,j,m,k}, q_{i,j,m,k}, g_{i,j,k}, g^{gfu}_{i,j,k}, e^{in}_{n,k}, g^{in}_{n,k}, \psi_n]$. The MP subjects to (13), (27), (32), (33), (37), and (39)–(44), and the Benders cuts from the SPs. The Benders cuts are initialized with $\psi_n \geq 0$, and are further supplemented by steps 4–6.

Denote the solution of MP in the sth iteration as $\hat{\mathbf{y}}^{(s)}$, and the value of the objective function as $\hat{\psi}^{(s)}$. Update $LB^{(s)} = \max\{LB^{(s-1)}, \hat{\psi}^{(s)}\}$.

3) Check the Feasibility of the Relaxed SP: The following relaxed SP for each EH is formulated and solved in parallel, given the solutions $\hat{e}^{in,(s)}_{n,k}$, $\hat{g}^{in,(s)}_{n,k}$ from MP

$$\underset{\mathbf{x}_{n,k}}{\mathrm{Min}} \quad \psi_n = C^{nd}_{n} + C^{rd}_{n} \tag{48}$$

which subjects to (2)–(24). The integer variables in (14) are relaxed into

$$0 \leq sw^{l}_{k,k'} \leq 1, sw^{l}_{k,k'} \in \mathbb{R}. \tag{49}$$

The relaxed SP is a linear programming problem, which can be easily checked for feasibility. If infeasible, go to step 4. Otherwise, obtain the solution $\hat{\mathbf{x}}^{(s)}_{n,k}$, and go to step 5.

4) Add Feasibility Cut to the MP: Get the Farkas dual variables λ of each relaxed SP. Denote the constraints of the SP in a compact form

$$\widetilde{\mathbf{A}}^{T}\left[\mathbf{x}_n \quad \mathbf{e}^{in}_{n} \quad \mathbf{g}^{in}_{n}\right] \leq \mathbf{b} \tag{50}$$

where $\widetilde{\mathbf{A}} = [\mathbf{A} \mid \mathbf{A}_{e^{in}} \quad \mathbf{A}_{g^{in}}]$. Then, the following feasibility cut (44) is provided to the MP. Go to step 2 to start the next Benders iteration

$$\lambda\left[\mathbf{A}_{e^{in}} \quad \mathbf{A}_{g^{in}}\right]^{T}\left[\mathbf{e}^{in}_{n} \quad \mathbf{g}^{inT}_{n}\right] \leq \lambda\mathbf{b}. \tag{51}$$

5) Check the Feasibility of the Energy Substitution SP: The energy substitution SP is formulated as

$$\underset{\mathbf{x}^{st}_{n}}{\mathrm{Min}} \quad \{0 | \text{s.t. } (2)-(12)\}. \tag{52}$$

The variables $\mathbf{x}^{nd}$ and $\mathbf{x}^{rd}$ are set to zero. If (52) is feasible, provide the optimality cut (53) to the MP, and go to step 1. Otherwise, go to step 6

$$\psi_n \geq \lambda \mathbf{b} - \lambda \left[\mathbf{A}_{e^{in}} \quad \mathbf{A}_{g^{in}}\right]^T \left[\mathbf{e}_n^{in} \quad \mathbf{g}_n^{in}\right]^T. \tag{53}$$

6) Add L&P Cut to the Relaxed SP: For each integer variable $sw_{k,k'}^{l}$, if the solution $\hat{\mathrm{sw}}_{k,k'}^{l,(s)}$ in the relaxed SP is fractional, then formulate the following L&P cut generating problem [53]:

$$\underset{\alpha_{e^{in}}, \alpha_{g^{in}}, \alpha_x, \beta}{\text{Min}} \quad \alpha_{e^{in}} \hat{e}_n^{in} + \alpha_{g^{in}} \hat{g}_n^{in} + \alpha_x \hat{\mathbf{x}}_n - \beta \tag{54}$$

s.t.

$$\alpha = \mathbf{u}^T \widetilde{\mathbf{A}} - u_0 \varepsilon_r \tag{55}$$

$$\alpha = \mathbf{v}^T \widetilde{\mathbf{A}} + v_0 \varepsilon_r \tag{56}$$

$$\alpha = [\alpha_x \ \alpha_{e^{in}} \ \alpha_{g^{in}}]^T \tag{57}$$

$$\beta = u^T b \tag{58}$$

$$\beta = v^T b + v_0 \tag{59}$$

$$\mathbf{1}^T \mathbf{u} + \mathbf{1}^T \mathbf{v} + u_0 + v_0 = 1 \tag{60}$$

$$u, v, u_0, v_0 \geq 0 \tag{61}$$

where r is the order of this integer variable among all the variables; and ε is the unit vector. The optimal solution $\hat{\alpha}_{e^{in}}^{(s,r)}$, $\hat{\alpha}_{g^{in}}^{(s,r)}$, $\hat{\alpha}_x^{(s,r)}$, and $\hat{\beta}^{(s,r)}$ can be obtained by solving the problem (54)–(61).

The relaxed SP in step 3 can be then updated by supplementing the L&P cut (62)

$$\hat{\alpha}_{e^{in}}^{(s,r)} \hat{e}_n^{in} + \hat{\alpha}_{g^{in}}^{(s,r)} \hat{g}_n^{in} + \hat{\alpha}_x^{(s,r)} \mathbf{x}_n - \hat{\beta}^{(s,r)} \geq 0. \tag{62}$$

Solve the updated relaxed SP. If feasible, provide the optimality cut to the MP, similar to (53). Otherwise, add feasibility cut similar to (51). Then, the upper bound can be updated as

$$UB^{(s)} = \min \left\{ UB^{(s-1)}, C^{E,(s)} + \sum_{n \in \mathrm{EH}} \hat{\psi}_n^{(s)} \right\}. \tag{63}$$

7) Convergence: Repeat the iteration from step 2 until the condition $(\mathrm{UB} - \mathrm{LB})/(\mathrm{UB} + \mathrm{LB}) < \delta$ is satisfied.

To sum up, the basic idea of the enhanced Benders decomposition procedure is that the load shifting-curtailing SP will only be checked when both the relaxed SP is feasible and the energy substitution SP is infeasible. With this checking mechanism, the complex loop 2, as in Fig. 4, can be replaced by the simpler loop 1 for most of the scenarios. Therefore, the computation efficiency can be significantly improved.

VI. Case Studies

A. Test System

In this section, an IEEE 24-bus Reliability Test System [54] and Belgium natural gas transmission system [55] are integrated to validate the proposed method. The two systems are topologically connected by GFUs and EHs, as presented in Fig. 6. The oil steam generating units with generation capacities of 12 MW, 20 MW, and 100 MW at electricity buses 15, 13, 14, and 2 are replaced by GFUs. The heat rate

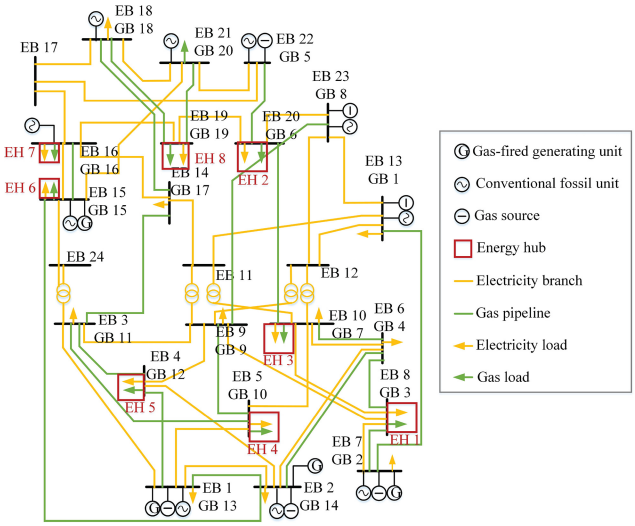

Fig. 6. Integrated electricity and gas test system with networked EHs.

coefficients of GFUs and gas production prices of gas sources are set according to [56]. The configuration of EHs is the same as that in Fig. 1. It is assumed that half of the electricity load at peak hours is supplied by EHs. Based on that, the electricity, heating, and cooling loads, as well as the capacities of the devices in the EHs, are normalized according to [57]. The energy conversion efficiencies of the devices in the EHs are also set according to [57]. The proportions of the shiftable and curtailable loads are set to 20% and 10%, respectively [58].

The numerical simulations are performed on a laptop with an Intel Core i7-8565U 1.80 GHz and a 16-GB memory. The optimization problems are solved using Gurobi. The self-scheduling SPs of EHs are parallelly processed by four cores.

B. Effectiveness of the Optimal Control for DR

In this section, a large requirement for DR capacity is set to validate the effectiveness of the proposed multilevel self-scheduling strategy in stressful scenarios. In other words, it should be ensured that the needs of energy end users can still be satisfied with reduced electricity consumption, without violating the physical constraints of devices (e.g., the electricity generating capacity of CHP). The peak value of the electricity load is increased by 0.3 times compared with the original Reliability Test System. The nodal gas pressures are limited to [0.95, 1.05] times of their values in the normal operating state. The DR signal is sent at 12:00. The DR period is set as 13:30–15:00. The available shifting-in period is set as 12:00–13:30 and 15:00–17:00. The DR capacity requirement is set based on the shortage of system reserve, e.g., 21.96 MW for EH 5.

The electricity and gas consumptions of EH 5 before and after self-scheduling are compared in Fig. 7(b) and (c). During 13:30–14:30, the energy of electricity consumption reduced by DR is 60.34 MWh. The detailed self-scheduling process of the electricity load in EH 5 is explicated in Fig. 7(a). It can be found that the load shifting and curtailment only account for 9.66 and 4.39 MWh, respectively. Most of the DR capacity is provided by energy substitution. The shifted-out

TABLE II
OPERATING COSTS AND LOAD SHIFTINGS/CURTAILMENTS WITH/WITHOUT LINEPACK UNDER DIFFERENT DR REQUIREMENTS

Gas pressure fluctuation limit (%)		1.2%	1.5%		
Required DR capacity (%)		10%	10%	30%	70%
with linepack	Operating cost ($)	2.59×10^5	2.52×10^5	2.53×10^5	2.57×10^5
	Electricity load shifting/curtailment (MWh)	0	0	0	0
without linepack	Operating cost ($)	Infeasible	2.52×10^5	2.59×10^5	6.36×10^6
	Electricity load shifting/curtailment (MWh)	Infeasible	0	15.03	131.51

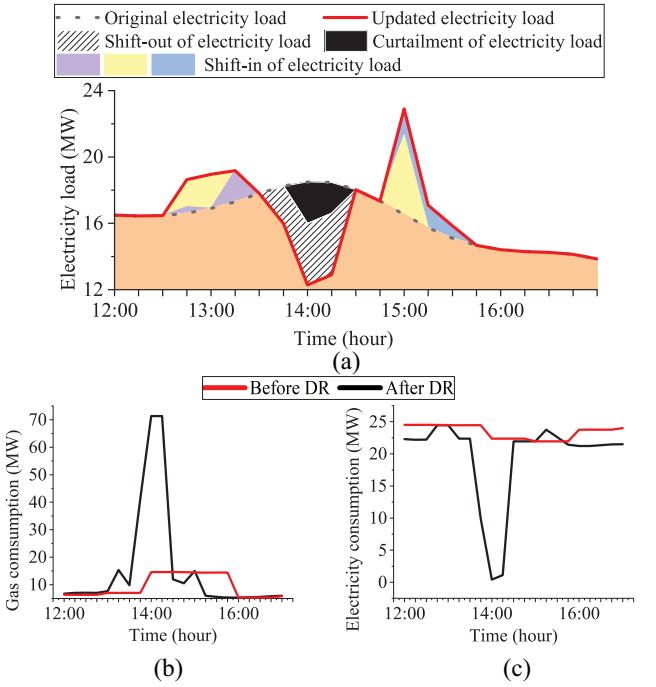

Fig. 7. (a) Shifting and curtailment of electricity load under a high stressed case. (b) Gas consumptions of the EH. (c) Electricity consumptions of the EH.

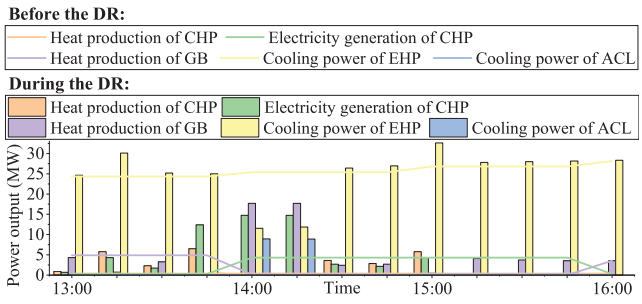

Fig. 8. Comparison of the operating conditions of EHs before and after DR.

electricity loads are deployed to the adjacent periods, such as 12:45–13:15 and 15:00–15:45. These shift-in loads are well accommodated by the remaining capacities of the EH during these periods, without increasing the electricity consumption.

Fig. 8 shows the realization of the energy substitution from the perspective of specific devices in the EH. During the DR period 13:30–15:00, the outputs of electricity-consuming devices (e.g., EHP) are generally replaced by gas-consuming devices (e.g., CHP, GBL, and ACL). Therefore, the gas consumption of the EH increases significantly during 14:00–14:30, as presented in Fig. 7(b).

TABLE III
COMPARISON OF COMPUTATION TIMES IN DIFFERENT SCENARIOS WITH DIFFERENT SOLUTION METHODS

	Scenario A	Scenario B	Scenario C
Method A	83 s	119 s	2055 s
Method B	4833 s	Do not converge within a reasonable time	Do not converge within a reasonable time
Method C	1822 s	2091 s	2303 s

To observe the impact of gas demand spikes on the IEGS operation, the gas pressures along the critical pipeline route (e.g., the pipelines passing through GBs 5, 6, 7, 4, 14, 13, 12, 11, 17, and 18) are presented in Fig. 9. The variations of gas pressures at critical GBs along the route during the DR period are presented in detail. It can be seen that the gas pressures are controlled strictly and smoothly between the upper and lower bounds. For example, GB 6 is connected to EH 2. The EH's gas consumption increases dramatically during the DR. To deliver that, the gas source at upstream GB 5 ramps up its gas production to increase the linepack. The nodal pressure of GB 5 also increases to prepare for the DR. Therefore, the increased gas consumption during DR can be well accommodated by the coordinated optimal control of IEGS and EHs.

C. Validation of Proposed Methods

The proposed DR framework and solution method are validated in this section by performing two comparative studies.

First, to validate the effectiveness of linepack utilization in the DR, we set two scenarios. One uses the linepack flexibilities to provide DR service, and the other does not use the linepack. The operating costs and load shifting/curtailment values in both scenarios with different DR requirements and gas pressure fluctuation limits are presented in Table II.

As we can see, when the gas pressure fluctuation limit is set to 1.2%, the EHs are not able to provide the 10% DR capacity if the linepack is not used. They can provide the DR only when the gas pressure fluctuation limit increases to 1.5%. This is because, without the linepack, the EH can only utilize the extra gas that is caused by the difference between the day-ahead schedule and intraday operation. This part of the gas is not adequate to cover the gas demand spike during the DR. Comparing different DR capacities, we find that when the DR capacity is low, the costs in the two scenarios are the same. There is no load shifting or curtailment in both scenarios. When the DR capacity increases, the operating cost and load shifting/curtailment without linepack are larger than those with linepack. This validates that using linepack is beneficial for DR, especially in stressed scenarios.

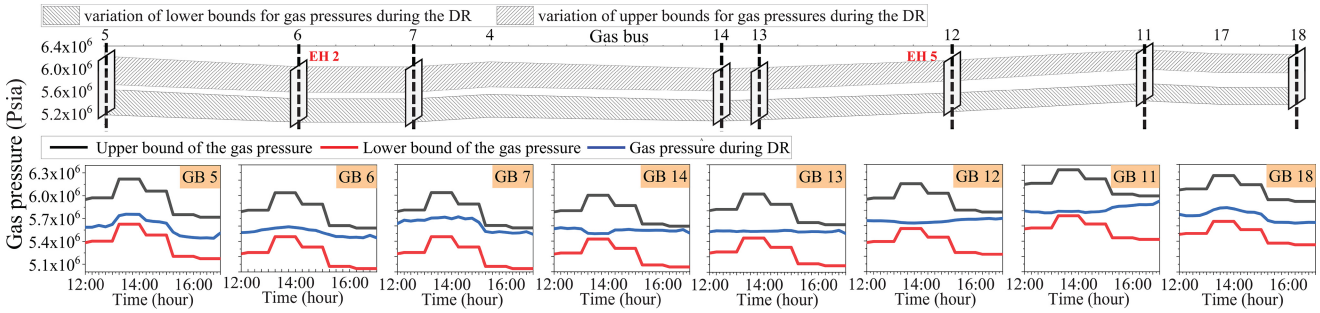

Fig. 9. Fluctuations of nodal gas pressures during DR.

TABLE IV
OPERATING CONDITION OF IEGS AND EHS WITH DIFFERENT DR SETTINGS

Gas pressure fluctuation limit (%)	1.20%					1.30%	2.40%	0.50%
DR duration (h),	1.5	1.5	1.5	0.5	5	1.5	1.5	Infeasible
DR capacity (%)	70%	40%	10%	70%	70%	70%	70%	
Total operating cost ($)	2.64×10^5	2.60×10^5	2.59×10^5	2.60×10^5	2.85×10^5	2.51×10^5	2.44×10^5	
Generation cost ($)	1.89×10^5	1.91×10^5	1.92×10^5	1.91×10^5	1.84×10^5	1.91×10^5	1.88×10^5	
Gas purchasing cost ($)	7.43×10^4	6.91×10^4	6.63×10^4	6.87×10^5	1.00×10^5	6.08×10^4	5.39×10^4	
Load shifting/curtailment (MW)	25.97	8.02	0	0	40.99	8.97	0	

Second, to demonstrate the effectiveness of the proposed EBD solution method, we set three scenarios A, B, and C, namely, the high-stress scenario, mid-stress scenario, and low-stress scenario. The DR durations in three scenarios are all set to 1.5 h, while the DR capacities are set to 10%, 50%, and 90% of the maximum DR potential, respectively. Three methods A, B, and C are used to solve the optimization problem in these scenarios. Method A is our proposed EBD method. In method B, the problem retains the nonlinearities in the self-scheduling and gas flow dynamics equations. Then, it is a large-scale mixed-integer nonlinear programming problem and is solved by using the Gurobi solver in a centralized manner. In method C, the reformulations are performed. Then, the original optimization problem becomes a large-scale mixed-integer SOC programming problem and is solved by using the Gurobi solver in a centralized manner. The tolerances of the gap in the three scenarios are all set to 10^{-3}.

The computation times are presented in Table III. As we can see, the proposed EBD method (method A) has the best performance in all three scenarios. The computation efficiency of the proposed method in scenario A is 98.28% and 95.44% higher than methods B and C, respectively. In scenarios B and C, as the requirement for DR capacity becomes larger, the computation time of our proposed method increases, especially in scenario C. This is because scenarios A and B only entail the energy substitution strategy, but the load-shifting strategy is evolved in scenario C. Then, the solution procedure enters loop 2, as shown in Fig. 6, which will take more time. Nonetheless, the computation time of the proposed method is controlled within the acceptable range. In contrast, method B cannot converge in Scenario B and C. It validates that the proposed method improves the tractability of the problem, which is more robust to stressed scenarios.

The computation time of our method in scenario C is further elaborated in Fig. 10. The IEGS MP occupies most of the computation time, while the parallel computing of the EH subproblem saves considerable time. Moreover, most of the Benders cuts at the beginning are generated by solving the linear programming problem instead of the mixed-integer linear programming problem, which also saves time. Judging from the computation time in our study, scenarios A and B can be implemented in the real-time or intraday market, while the implementation of scenario C should be notified ahead of time. This is reasonable because when more DR services are required, the EHs need more time to get prepared.

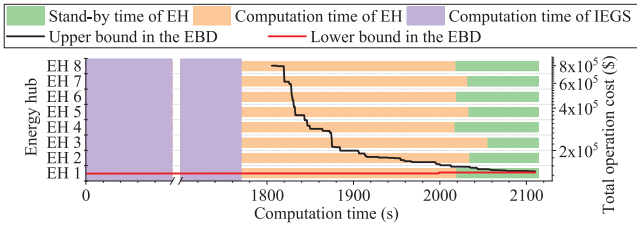

Fig. 10. Computation time of proposed solution strategy.

D. Comparisons of Various DR Requirements

Though the self-scheduling of EHs does not violate the IEGS security constraints, the fluctuation of gas pressure and utilization of linepack may still put the IEGS in a vulnerable state against future risks (e.g., load volatility or component failures). Therefore, it should be ensured that the side effect of self-scheduling (i.e., spikes in gas consumption from the natural gas transmission system) can be well accommodated by linepack flexibilities by using our proposed coordinated control framework. It means that although gas consumption increases dramatically, the gas system still operates normally, and all the physical states (such as gas pressure, gas flow, etc.) are limited by their physical constraints. To this end, key factors, such as the DR capacity, operating cost, and gas pressure fluctuations should be balanced. For further investigation, the operating conditions of EHs and IEGS

$$\mathbf{H}=\begin{bmatrix}
0 & 0 & 1 & 0 & 0 & 1 & 0 & 0 & 0 & 0 & 0 & 0 & 0 & 0 & 0 \\
0 & 0 & 0 & 0 & 0 & 0 & 0 & 0 & 1 & 1 & 0 & 0 & 1 & 0 & 0 \\
0 & 0 & 0 & 0 & 0 & 0 & 0 & 0 & 0 & 0 & 0 & 0 & 0 & 1 & 1 \\
1 & 0 & -1 & -1 & 0 & 0 & 0 & 0 & 0 & 0 & 0 & 0 & 0 & 0 & 0 \\
0 & 1 & 0 & 0 & 0 & 0 & -1 & -1 & 0 & 0 & 0 & 0 & 0 & 0 & 0 \\
0 & 0 & 0 & \mathrm{COP}_3^h\gamma & \mathrm{COP}_3^h\gamma & 0 & 0 & 0 & -1 & 0 & 0 & 0 & 0 & 0 & 0 \\
0 & 0 & 0 & \mathrm{COP}_3^c(1-\gamma) & \mathrm{COP}_3^c(1-\gamma) & 0 & 0 & 0 & 0 & 0 & 0 & 0 & 0 & -1 & 0 \\
0 & 0 & 0 & 0 & -1 & -1 & \eta_1^e & 0 & 0 & 0 & 0 & 0 & 0 & 0 & 0 \\
0 & 0 & 0 & 0 & 0 & 0 & \eta_1^h & 0 & 0 & -1 & -1 & 0 & 0 & 0 & 0 \\
0 & 0 & 0 & 0 & 0 & 0 & 0 & \eta_2 & 0 & 0 & 0 & -1 & -1 & 0 & 0 \\
0 & 0 & 0 & 0 & 0 & 0 & 0 & 0 & 0 & 0 & \mathrm{COP}_4 & \mathrm{COP}_4 & 0 & 0 & -1
\end{bmatrix} \tag{64}$$

with various DR requirements, including DR capacities, DR durations, and gas pressure fluctuation limits are compared

The simulation results are presented in Table IV. In the scenarios with the gas pressure fluctuation limits of 1.20%, the total operating cost, gas purchasing cost, and load shifting/curtailment are higher with the increase of the DR capacity and DR duration. By contrast, the generation cost is reduced, because the reserves are covered in part by the DR of EHs. With the relaxation of gas pressure limits from 1.20% to 1.30% and 2.40%, the EHs tend to have more flexibility to perform self-scheduling, and thus the total operating cost and load shifting/curtailment can be reduced.

VII. Conclusion

This article proposes a coordinated optimal control framework of IEGS and EHs for providing DR services. A multilevel self-scheduling for the EH is developed by incorporating energy substitution, temporal load shifting, and load curtailment strategies. The gas flow dynamics of the linepack are utilized to accommodate gas demand spikes. To solve the optimal control problem, reformulation techniques are used to convexify both the load shifting and motion equations. The Benders decomposition is also enhanced with the L&P cutting plane method to solve this large-scale mixed-integer SOC programming problem in a decentralized manner. A unique solution procedure is further devised to reduce the computation burden.

The results verify that even under a highly stressed situation, the EHs can still demonstrate great potential for DR with the proposed method, which can achieve about 3 times of electricity reduction compared with that in traditional electricity DR. The fluctuation of nodal gas pressure can be also controlled within an appropriate range (e.g., 1.20%). This article can assist the IEGS operators in devising the coordination strategies between the electricity and gas systems during the operational phase.

Apart from the solution tractability and privacy-preserving issues addressed in this article, with the ever-increasing integration of distributed flexible resources (such as electrical vehicles, air conditioners, and distributed wind generators), the energy system is still facing challenges in real-time operations. The first one is the increasing communication burdens due to large data transmission volumes, which could lead to issues like package drop and communication latency. New technologies, such as consensus control, federated learning, and cloud–edge computing, are essential to address these based on a more decentralized structure. Second, as EHs are gradually transferred from pure consumers to prosumers, packaging the distributed resources as a virtual power plant shows promising arbitrage potential in ancillary markets. To deal with the heterogeneous physical/economic characteristics of distributed resources, the bidding strategies on the ancillary market should be well-tailored based on unique operating characteristics and marginal costs. Third, more sophisticated operation schemes should be devised using model predictive control, distributionally robust optimization, chance constraints, etc., to hedge against various uncertainties, such as weather, load, and energy price in future works.

Appendix
Sparse Energy Conversion Matrix

The specific formulation of the sparse energy conversion matrix is presented in (64), as shown at the top of the page, where COP_3^h and COP_3^c are the coefficients of performance of the EHP in heating and cooling mode, respectively; γ is the indicator for EHP operating mode, where $\gamma = 1$ represents heating mode, and $\gamma = 0$ represents cooling mode; η_1^e and η_1^h are the electrical and thermal efficiencies of the CHP, respectively; η_2 is the thermal efficiency of the GBL; and COP_4 is the coefficient of performance of the ACL.

References

[1] H. Li, Z. Ren, A. Trivedi, D. Srinivasan, and P. Liu, "Optimal planning of dual-zero microgrid on an island towards net-zero carbon emission," *IEEE Trans. Smart Grid*, early access, Jul. 28, 2023, doi: 10.1109/TSG.2023.3299639.

[2] G. Xu, W. Yu, D. Griffith, N. Golmie, and P. Moulema, "Toward integrating distributed energy resources and storage devices in smart grid," *IEEE Internet Things J.*, vol. 4, no. 1, pp. 192–204, Feb. 2017.

[3] M. Geidl, G. Koeppel, P. Favre-Perrod, and B. Klockl, "Energy hubs for the future," *IEEE Power Energy Mag.*, vol. 5, no. 1, pp. 24–30, Jan./Feb. 2007.

[4] S. Wang, H. Hui, Y. Ding, C. Ye, and M. Zheng, "Operational reliability evaluation of urban multi-energy systems with equivalent energy storage," *IEEE Trans. Ind. Appl.*, vol. 59, no. 2, pp. 2186–2201, Mar./Apr. 2023.

[5] C. Shao, Y. Ding, J. Wang, and Y. Song, "Modeling and integration of flexible demand in heat and electricity integrated energy system," *IEEE Trans. Sustain. Energy*, vol. 9, no. 1, pp. 361–370, Jul. 2018.

[6] I. G. Moghaddam, M. Saniei, and E. Mashhour, "A comprehensive model for self-scheduling an energy hub to supply cooling, heating and electrical demands of a building," *Energy*, vol. 94, pp. 157–170, Jan. 2016.

[7] A. Sheikhi, M. Rayati, S. Bahrami, and A. M. Ranjbar, "Integrated demand side management game in smart energy hubs," *IEEE Trans. Smart Grid*, vol. 6, no. 2, pp. 675–683, Mar. 2015.

[8] M. Aghamohamadi, M. E. Hajiabadi, and M. Samadi, "A novel approach to multi energy system operation in response to DR programs; an application to incentive-based and time-based schemes," *Energy*, vol. 156, pp. 534–547, Aug. 2018.

[9] S. A. Mansouri, A. Ahmarinejad, M. Ansarian, M. S. Javadi, and J. P. S. Catalao, "Stochastic planning and operation of energy hubs considering demand response programs using Benders decomposition approach," *Int. J. Electr. Power Energy Syst.*, vol. 120, Sep. 2020, At. no. 106030.

[10] M. Z. Oskouei, B. Mohammadi-Ivatloo, M. Abapour, M. Shafiee, and A. Anvari-Moghaddam, "Privacy-preserving mechanism for collaborative operation of high-renewable power systems and industrial energy hubs," *Appl. Energy*, vol. 283, Feb. 2021, Art. no. 116338.

[11] M. Aghamohamadi, A. Mahmoudi, J. K. Ward, M. H. Haque, and J. P. S. Catalão, "A block-coordinate-descent robust approach to incentive-based integrated demand response in managing multienergy hubs with must-run processes," *IEEE Trans. Ind. Appl.*, vol. 58, no. 2, pp. 2352–2368, Mar./Apr. 2022.

[12] J. Ramos-Teodoro, F. Rodríguez, M. Berenguel, and J. L. Torres, "Heterogeneous resource management in energy hubs with self-consumption: Contributions and application example," *Appl. Energy*, vol. 229, pp. 537–550, Nov. 2018.

[13] T. Zhao, Y. Li, X. Pan, P. Wang, and J. Zhang, "Real-time optimal energy and reserve management of electric vehicle fast charging station: Hierarchical game approach," *IEEE Trans. Smart Grid*, vol. 9, no. 5, pp. 5357–5370, Sep. 2018.

[14] H. Hui et al., "A transactive energy framework for inverter-based HVAC loads in a real-time local electricity market considering distributed energy resources," *IEEE Trans. Ind. Informat.*, vol. 18, no. 12, pp. 8409–8421, Dec. 2022.

[15] H. Hui, Y. Ding, K. Luan, T. Chen, Y. Song, and S. Rahman, "Coupon-based demand response for consumers facing flat-rate retail pricing," *CSEE J. Power Energy Syst.*, early access, Apr. 20, 2023, doi: 10.17775/CSEEJPES.2021.05140.

[16] S. Bahrami and A. Sheikhi, "From demand response in smart grid toward integrated demand response in smart energy hub," *IEEE Trans. Smart Grid*, vol. 7, no. 2, pp. 650–658, Mar. 2016.

[17] C. Feng, B. Liang, Z. Li, W. Liu, and F. Wen, "Peer-to-peer energy trading under network constraints based on generalized fast dual ascent," *IEEE Trans. Smart Grid*, vol. 14, no. 2, pp. 1441–1453, Mar. 2023.

[18] P. Li et al., "Stochastic robust optimal operation of community integrated energy system based on integrated demand response," *Int. J. Electr. Power Energy Syst.*, vol. 128, Jun. 2021, Art. no. 106735.

[19] H. Qi, H. Yue, J. Zhang, and K. L. Lo, "Optimisation of a smart energy hub with integration of combined heat and power, demand side response and energy storage," *Energy*, vol. 234, Nov. 2021, Art. no. 121268.

[20] T. Liu, D. Zhang, H. Dai, and T. Wu, "Intelligent modeling and optimization for smart energy hub," *IEEE Trans. Ind. Electron.*, vol. 66, no. 12, pp. 9898–9908, Dec. 2019.

[21] B. Kazemi, A. Kavousi-Fard, M. Dabbaghjamanesh, and M. Karimi, "IoT-enabled operation of multi energy hubs considering electric vehicles and demand response," *IEEE Trans. Intell. Transp. Syst.*, vol. 24, no. 2, pp. 2668–2676, Feb. 2023.

[22] S. Clegg and P. Mancarella, "Integrated electrical and gas network flexibility assessment in low-carbon multi-energy systems," *IEEE Trans. Sustain. Energy*, vol. 7, no. 2, pp. 718–731, Apr. 2016.

[23] S. Wang, J. Zhai, H. Hui, Y. Ding, and Y. Song, "Operational reliability of integrated energy systems considering gas flow dynamics and demand-side flexibilities," *IEEE Trans. Ind. Informat.*, early access, May 12, 2023, doi: 10.1109/TII.2023.3275712.

[24] H. R. Massrur, T. Niknam, and M. Fotuhi-Firuzabad, "Investigation of carrier demand response uncertainty on energy flow of renewable-based integrated electricity–gas–heat systems," *IEEE Trans. Ind. Informat.*, vol. 14, no. 11, pp. 5133–5142, Nov. 2018.

[25] L. Ni et al., "Optimal operation of electricity, natural gas and heat systems considering integrated demand responses and diversified storage devices," *J. Mod. Power Syst. Clean Energy*, vol. 6, no. 3, pp. 423–437, May 2018.

[26] M. H. Shams, M. Shahabi, and M. E. Khodayar, "Stochastic day-ahead scheduling of multiple energy carrier microgrids with demand response," *Energy*, vol. 155, pp. 326–338, Jul. 2018.

[27] A. Dini, S. Pirouzi, M. Norouzi, and M. Lehtonen, "Grid-connected energy hubs in the coordinated multi-energy management based on day-ahead market framework," *Energy*, vol. 188, Sep. 2019, Art. no. 116055.

[28] H. Yang, P. You, and C. Shang, "Distributed planning of electricity and natural gas networks and energy hubs," *Appl. Energy*, vol. 282, Nov. 2021, Art. no. 116090.

[29] N. Jia, C. Wang, Y. Li, N. Liu, and T. Bi, "Two-stage robust dispatch of multi-area integrated electric-gas systems: A decentralized approach," *CSEE J. Power Energy Syst.*, early access, May 6, 2022, doi: 10.17775/CSEEJPES.2021.04010.

[30] H. Xie, X. Sun, C. Chen, Z. Bie, and J. P. S. Catal˜o, "Resilience metrics for integrated power and natural gas systems," *IEEE Trans. Smart Grid*, vol. 13, no. 3, pp. 2483–2486, May 2022.

[31] J. Yang, N. Zhang, C. Kang, and Q. Xia, "Effect of natural gas flow dynamics in robust generation scheduling under wind uncertainty," *IEEE Trans. Power Syst.*, vol. 33, no. 2, pp. 2087–2097, Mar. 2018.

[32] D. Huo, C. Gu, K. Ma, W. Wei, Y. Xiang, and S. L. Blond, "Chance-constrained optimization for multienergy hub systems in a smart city," *IEEE Trans. Ind. Electron.*, vol. 66, no. 2, pp. 1402–1412, Feb. 2019.

[33] W. Zhuang, S. Zhou, W. Gu, and X. Chen, "Optimized dispatching of city-scale integrated energy system considering the flexibilities of city gas gate station and line packing," *Appl. Energy*, vol. 290, May 2021, Art. no. 116689.

[34] A. Bostan, M. S. Nazar, M. Shafie-Khah, and J. P. S. Catalão, "Optimal scheduling of distribution systems considering multiple downward energy hubs and demand response programs," *Energy*, vol. 190, Oct. 2020, Art. no. 116349.

[35] Y. He et al., "Decentralized optimization of multi-area electricity-natural gas flows based on cone reformulation," *IEEE Trans. Power Syst.*, vol. 33, no. 4, pp. 4531–4542, Jul. 2018.

[36] Y. Li, Z. Li, F. Wen, and M. Shahidehpour, "Privacy-preserving optimal dispatch for an integrated power distribution and natural gas system in networked energy hubs," *IEEE Trans. Sustain. Energy*, vol. 10, no. 4, pp. 2028–2038, Oct. 2019.

[37] M. Yan, Y. He, M. Shahidehpour, X. Ai, Z. Li, and J. Wen, "Coordinated regional-district operation of integrated energy systems for resilience enhancement in natural disasters," *IEEE Trans. Smart Grid*, vol. 10, no. 5, pp. 4881–4892, Sep. 2019.

[38] Y. Chen, L. Xu, A. Egea-Àlvarez, and B. Marshall, "Accurate and general small-signal impedance model of LCC-HVDC in sequence frame," *IEEE Trans. Power Del.*, to be published.

[39] C. Shao, Y. Ding, P. Siano, and Z. Lin, "A framework for incorporating demand response of smart buildings into the integrated heat and electricity energy system," *IEEE Trans. Ind. Electron.*, vol. 66, no. 2, pp. 1465–1475, Feb. 2019.

[40] Y. Tao, J. Qiu, and S. Lai, "A hybrid cloud and edge control strategy for demand responses using deep reinforcement learning and transfer learning," *IEEE Trans. Cloud Comput.*, vol. 10, no. 1, pp. 56–71, Jan.–Mar. 2022.

[41] S. Yang, K.-W. Lao, H. Hui, Y. Chen, and N. Dai, "Real-time harmonic contribution evaluation considering multiple dynamic customers," *CSEE J. Power Energy Syst.*, early access, Apr. 20, 2023, doi: 10.17775/CSEEJPES.2022.06570.

[42] S. Yang, K.-W. Lao, Y. Chen, and H. Hui, "Resilient distributed control against false data injection attacks for demand response," *IEEE Trans. Power Syst.*, early access, Jun. 19, 2023, doi: 10.1109/TPWRS.2023.3287205.

[43] J. Su, H. Zhang, H. Liu, L. Yu, and Z. Tan, "Membership-function-based secondary frequency regulation for distributed energy resources in islanded microgrids with communication delay compensation," *IEEE Trans. Sustain. Energy*, vol. 14, no. 4, pp. 2274–2293, Oct. 2023.

[44] T. Jiang, H. Deng, L. Bai, R. Zhang, X. Li, and H. Chen, "Optimal energy flow and nodal energy pricing in carbon emission-embedded integrated energy systems," *CSEE J. Power Energy Syst.*, vol. 4, no. 2, pp. 179–187, Jun. 2018.

[45] G. Wacker and R. Billinton, "Customer cost of electric service interruptions," *Proc. IEEE*, vol. 77, no. 6, pp. 919–930, Jun. 1989.

[46] A. Helseth and A. T. Holen, "Impact of energy end use and customer interruption cost on optimal allocation of switchgear in constrained distribution networks," *IEEE Trans. Power Del.*, vol. 23, no. 3, pp. 1419–1425, Jul. 2008.

[47] H. Zhou, Z. Li, J. H. Zheng, Q. H. Wu, and H. Zhang, "Robust scheduling of integrated electricity and heating system hedging heating network uncertainties," *IEEE Trans. Smart Grid*, vol. 11, no. 2, pp. 1543–1555, Mar. 2020.
[48] S. Wang, J. Zhai, and H. Hui, "Optimal energy flow in integrated electricity and gas systems with injection of alternative gas," *IEEE Trans. Sustain. Energy*, vol. 14, no. 3, pp. 1540–1557, Jan. 2023.
[49] I. Cameron, "Using an excel-based model for steady-state and transient simulation," in *Proc. PSIG Annu. Meeting*, 1999, p. 39.
[50] A. Herrán-González, J. M. De La Cruz, B. De Andrés-Toro, and J. L. Risco-Martín, "Modeling and simulation of a gas distribution pipeline network," *Appl. Math. Model.*, vol. 33, no. 3, pp. 1584–1600, Mar. 2009.
[51] Y. Zhou, C. Gu, H. Wu, and Y. Song, "An equivalent model of gas networks for dynamic analysis of gas-electricity systems," *IEEE Trans. Power Syst.*, vol. 32, no. 6, pp. 4255–4264, Nov. 2017.
[52] H. Li, Q. Wu, L. Yang, H. Zhang, and S. Jiang, "Distributionally robust negative-emission optimal energy scheduling for off-grid integrated electricity-heat microgrid," *IEEE Trans. Sustain. Energy*, early access, Aug. 18, 2023, doi: 10.1109/TSTE.2023.3306360.
[53] C. Li and I. E. Grossmann, "A generalized benders decomposition-based branch and cut algorithm for two-stage stochastic programs with nonconvex constraints and mixed-binary first and second stage variables," *J. Global Optim.*, vol. 75, no. 2, pp. 247–272, Oct. 2019.
[54] C. Grigg et al., "The IEEE reliability test system-1996. A report prepared by the reliability test system task force of the application of probability methods subcommittee," *IEEE Trans. Power Syst.*, vol. 14, no. 3, pp. 1010–1020, Aug. 1999.
[55] S. Wang, Y. Ding, C. Ye, C. Wan, and Y. Mo, "Reliability evaluation of integrated electricity–gas system utilizing network equivalent and integrated optimal power flow techniques," *J. Mod. Power Syst. Clean Energy*, vol. 7, no. 6, pp. 1523–1535, Nov. 2019.
[56] C. Unsihuay, J. W. M. Lima, and A. C. Z. de Souza, "Modeling the integrated natural gas and electricity optimal power flow," in *Proc. IEEE Power Eng. Soc. Gen. Meeting*, 2007, pp. 1–7.
[57] P. Mancarella and G. Chicco, "Real-time demand response from energy shifting in distributed multi-generation," *IEEE Trans. Smart Grid*, vol. 4, no. 4, pp. 1928–1938, Dec. 2013.
[58] S. Wang, C. Shao, Y. Ding, and J. Yan, "Operational reliability of multi-energy customers considering service-based self-scheduling," *Appl. Energy*, vol. 254, Nov. 2019, Art. no. 113531.

Sheng Wang (Member, IEEE) received the B.Eng. and Ph.D. degrees in electrical engineering from Zhejiang University, Hangzhou, China, in 2016 and 2021, respectively.

He was with State Grid (Suzhou) City Energy Research Institute, Suzhou, China, in 2021. He is currently a Postdoctoral Fellow with the State Key Laboratory of Internet of Things for Smart City, University of Macau, Macau, China. His research interests include the optimization and reliability evaluation of low-carbon energy systems.

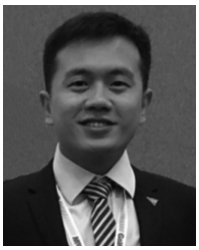

Hongxun Hui (Member, IEEE) received the B.E. and Ph.D. degrees in electrical engineering from Zhejiang University, Hangzhou, China, in 2015 and 2020, respectively.

From 2018 to 2019, he was a Visiting Scholar with the Advanced Research Institute, Virginia Tech, Blacksburg, VA, USA, and the CURENT Center, University of Tennessee, Knoxville, TN, USA. He is currently a Research Assistant Professor with the State Key Laboratory of Internet of Things for Smart City, University of Macau, Macau, SAR, China. His research interests include optimization and control of power system, demand response, and Internet of Things technologies for smart energy.

Yi Ding (Member, IEEE) received the bachelor's degree in electrical engineering from Shanghai Jiaotong University, Shanghai, China, in 2000, and the Ph.D. degree in electrical engineering from Nanyang Technological University, Singapore, in 2007.

He is currently a Professor with the College of Electrical Engineering, Zhejiang University, Hangzhou, China. His research interests include power systems reliability and performance analysis incorporating renewable energy resources and engineering systems reliability modeling and optimization.

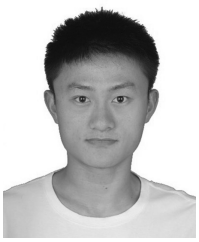

Junyi Zhai (Member, IEEE) received the B.S. and Ph.D. degrees in electrical engineering from North China Electricity Power University, Beijing, China, in 2014 and 2019, respectively.

He was a visiting student with the University of Birmingham, Birmingham, U.K., from 2018 to 2019. He was a Senior Research Engineer with State Grid (Suzhou) City Energy Research Institute, Suzhou, China, from 2019 to 2021. His research interests include mathematical optimization techniques and power system analysis and computing.